Yasuhiro Onogi,[1] Tsutomu Wada,[1] Chie Kamiya,[1] Kento Inata,[1] Takatoshi Matsuzawa,[1] Yuka Inaba,[2,3] Kumi Kimura,[2] Hiroshi Inoue,[2,3] Seiji Yamamoto,[4] Yoko Ishii,[4] Daisuke Koya,[5] Hiroshi Tsuneki,[1] Masakiyo Sasahara,[4] and Toshiyasu Sasaoka[1]

PDGFRβ Regulates Adipose Tissue Expansion and Glucose Metabolism via Vascular Remodeling in Diet-Induced Obesity

Diabetes 2017;66:1008–1021 | DOI: 10.2337/db16-0881

Platelet-derived growth factor (PDGF) is a key factor in angiogenesis; however, its role in adult obesity remains unclear. In order to clarify its pathophysiological role, we investigated the significance of PDGF receptor β (PDGFRβ) in adipose tissue expansion and glucose metabolism. Mature vessels in the epididymal white adipose tissue (eWAT) were tightly wrapped with pericytes in normal mice. Pericyte desorption from vessels and the subsequent proliferation of endothelial cells were markedly increased in the eWAT of diet-induced obese mice. Analyses with flow cytometry and adipose tissue cultures indicated that PDGF-B caused the detachment of pericytes from vessels in a concentration-dependent manner. M1-macrophages were a major type of cells expressing PDGF-B in obese adipose tissue. In contrast, pericyte detachment was attenuated and vascularity within eWAT was reduced in tamoxifen-inducible conditional *Pdgfrb*-knockout mice with decreases in adipocyte size and chronic inflammation. Furthermore, *Pdgfrb*-knockout mice showed enhanced energy expenditure. Consequently, diet-induced obesity and the associated deterioration of glucose metabolism in wild-type mice were absent in *Pdgfrb*-knockout mice. Therefore, PDGF-B–PDGFRβ signaling plays a significant role in the development of adipose tissue neovascularization and appears to be a fundamental target for the prevention of obesity and type 2 diabetes.

The physiological roles of the vasculature in adipose tissue have been attracting interest from the viewpoint of adipose tissue expansion and chronic inflammation (1,2). White adipose tissue (WAT) such as visceral fat possesses the unique characteristic of plasticity; its volume may change several fold even after growth depending on nutritional conditions. Enlarged adipose tissue is chronically exposed to hypoxia (3,4), which stimulates the production of angiogenic factors for the supplementation of nutrients and oxygen to the newly enlarged tissue area (5). Selective ablation of the vasculature in WAT by apoptosis-inducible peptides or the systemic administration of angiogenic inhibitors has been shown to reduce WAT volumes and result in better glucose metabolism profiles in obese mice (1,2,6). Regarding angiogenic factors, vascular endothelial growth factor (VEGF) has been characterized in the most detail and is known to play crucial roles in the neovascular development of adipose tissue with obesity (7–13).

PDGF-B is another growth factor and its homodimer activates an intracellular signaling cascade by binding to its receptor, PDGF receptor β (PDGFRβ) (14,15). It plays an essential role in fetal vascular development and also contributes to wound healing and tumor growth via angiogenic actions in adults (16). PDGFRβ is almost restrictively expressed in perivascular mesenchymal cells, particularly in vascular smooth muscle cells and pericytes

[1]Department of Clinical Pharmacology, University of Toyama, Toyama, Japan
[2]Department of Physiology and Metabolism, Brain/Liver Interface Medicine Research Center, Institute for Frontier Science Initiative, Kanazawa University, Ishikawa, Japan
[3]Metabolism and Nutrition Research Unit, Innovative Integrated Bio-Research Core, Institute for Frontier Science Initiative, Kanazawa University, Ishikawa, Japan
[4]Department of Pathology, University of Toyama, Toyama, Japan
[5]Department of Internal Medicine, Kanazawa Medical University, Ishikawa, Japan

Corresponding authors: Toshiyasu Sasaoka, tsasaoka@pha.u-toyama.ac.jp, and Tsutomu Wada, twada@pha.u-toyama.ac.jp.

Received 19 July 2016 and accepted 17 January 2017.

This article contains Supplementary Data online at http://diabetes.diabetesjournals.org/lookup/suppl/doi:10.2337/db16-0881/-/DC1.

(14,15). Endothelial cell (EC)–derived PDGF-B promotes the migration of pericytes to neovessels for maturation by covering blood vessels, and these pericytes regulate vascular permeability and sprouting (17). The systemic deletion of the *Pdgfb* or *Pdgfrb* gene results in a lack of pericytes in the vasculature and embryonic lethality with vascular dysfunction (15,18–20). However, it currently remains unclear whether the angiogenic effects of PDGF are involved in the mechanisms responsible for the development of adult obesity.

Therefore, we herein used tamoxifen-inducible conditional *Pdgfrb*-knockout (KO) mice in which PDGFRβ was deleted during adulthood without affecting vascular development in the fetal and growing periods for the selective ablation of *Pdgfrb*. These mice were fed a normal chow diet or a high-fat diet (HFD), and the effects of the *Pdgfrb* deletion on adipose tissue vasculature and glucose metabolism were investigated.

RESEARCH DESIGN AND METHODS

Materials

Human recombinant insulin was provided by Novo Nordisk Pharma Ltd. Antibodies and ELISA kits used in this study were listed in Supplementary Table 1. All other reagents of analytical grade not elsewhere specified were obtained from Sigma-Aldrich or Wako Pure Chemical Industries.

Mice and Metabolic Analyses

All experimental procedures used in this study were approved by the Committee of Animal Experiments at the University of Toyama. $Pdgfrb^{flox/flox}$ mice on a C57BL/6 background were crossbred with Cre-estrogen receptor transgenic mice (The Jackson Laboratory). Their offspring, Cre-ER/$Pdgfrb^{flox/flox}$, were orally administered tamoxifen at 9 weeks old (2.25 mg/10 g body wt for 5 consecutive days; Cayman) to produce conditional systemic $Pdgfrb^{\Delta SYS}$-KO mice, as shown in Fig. 1*E* (21,22). To conduct experiments appropriately, $Pdgfrb^{flox/flox}$ littermates of the same age and sex were treated identically and used as controls (FL). Mice were housed in a temperature-controlled colony room (23 ± 3°C) with free access to food and water under a 12-h light-dark cycle (lights on at 7:00 A.M.). Mice were fed control PicoLab Rodent Diet 20 (chow 3.43 kcal/g; PMI Nutrition International) or 60 kcal% HFD (5.24 kcal/g; D12492; Research Diets Inc.) for 12 weeks, and physiological experiments were performed thereafter. Male mice were used in all experiments. The glucose tolerance test (GTT) and insulin tolerance test (ITT) were conducted after 6 h of fasting, as described previously (23,24). Body composition was analyzed with MRI (MRmini SA; DS Pharma Biomedical, Osaka, Japan), as described previously (25,26).

Hyperinsulinemic-Euglycemic Clamp

Hyperinsulinemic-euglycemic clamp studies were performed after 7–8 days of recovery from cannulation, as described previously (27). During clamp studies, human insulin at a concentration of 2.5 mU/kg/min was infused into mice with variable amounts of the 40% glucose solution to maintain blood glucose levels at 110 ± 20 mg/dL.

Cell and Adipose Tissue Cultures

Bone marrow–derived macrophages (BMDMs) were prepared, as described previously (4). Bone marrow cells were treated with 100 nmol/L 4-hydroxytamoxifen to delete the *Pdgfrb* allele for 48 h and differentiated into FL-BMDM and *Pdgfrb*-KO-BMDM, respectively. In adipose tissue cultures, epididymal WAT (eWAT) isolated from lean 8- to 12-week-old male mice was cut into small pieces (~3 × 3 mm) and cultured in serum-free DMEM. To obtain *Pdgfrb*-KO tissue, adipose tissue pieces from Cre-ER/$Pdgfrb^{flox/flox}$ or $Pdgfrb^{flox/flox}$ control mice were incubated with 100 nmol/L 4-hydroxytamoxifen for 48 h. These adipose tissues were treated with or without PDGF-BB (Life Technologies) for 24 h and were used for the analysis of whole-mount immunofluorescence.

Immunofluorescence in Sections and Whole-Mount Adipose Tissue

Immunofluorescence analyses were performed in accordance with previous methods with minor modifications (28). Sections (30- or 40-μm slices) were obtained from the middle part of the eWAT using a cryostat (CM 3050S-IV; Leica Microsystems) and were used in experiments of Fig. 3*D* and *I*, and Supplementary Fig. 4*D*. To conduct whole-mount immunofluorescence, tissues obtained from the tip region of eWAT, an active area for neoangiogenesis (29), were stained with antibodies and subsequently incubated with fructose solution as an optical clearing agent to reduce the amount of light scattering in tissues (30) and were used in experiments shown in Fig. 3*A* and *F*. The immunofluorescent images were randomly obtained by a confocal microscope (TCS-SP5; Leica Microsystems). Blood vessel areas, pericyte association levels, and PDGFRβ-like immunoreactivities in each mouse were measured with the ImageJ software (National Institutes of Health), and the data were averaged.

Real-Time PCR and Western Blotting

The method used for real-time PCR and Western blotting was described previously (23). Primer sequences are listed in Supplementary Table 2.

Flow Cytometry

The fractionation of the stromal vascular fraction (SVF) of eWAT was analyzed by FACSCanto II and FACSAria II for cell sorting (BD Biosciences), as previously described (26,31). Data were analyzed by FACS Diva 6.1.2 (BD Biosciences) or FCS Express (De Novo Software).

Measurement of Energy Consumption and Locomotor Activity

VO_2, VCO_2, locomotor activity, and food consumption were measured with metabolic chambers (MK-5000RQ; Muromachi Kikai, Tokyo, Japan), as described previously (25,26).

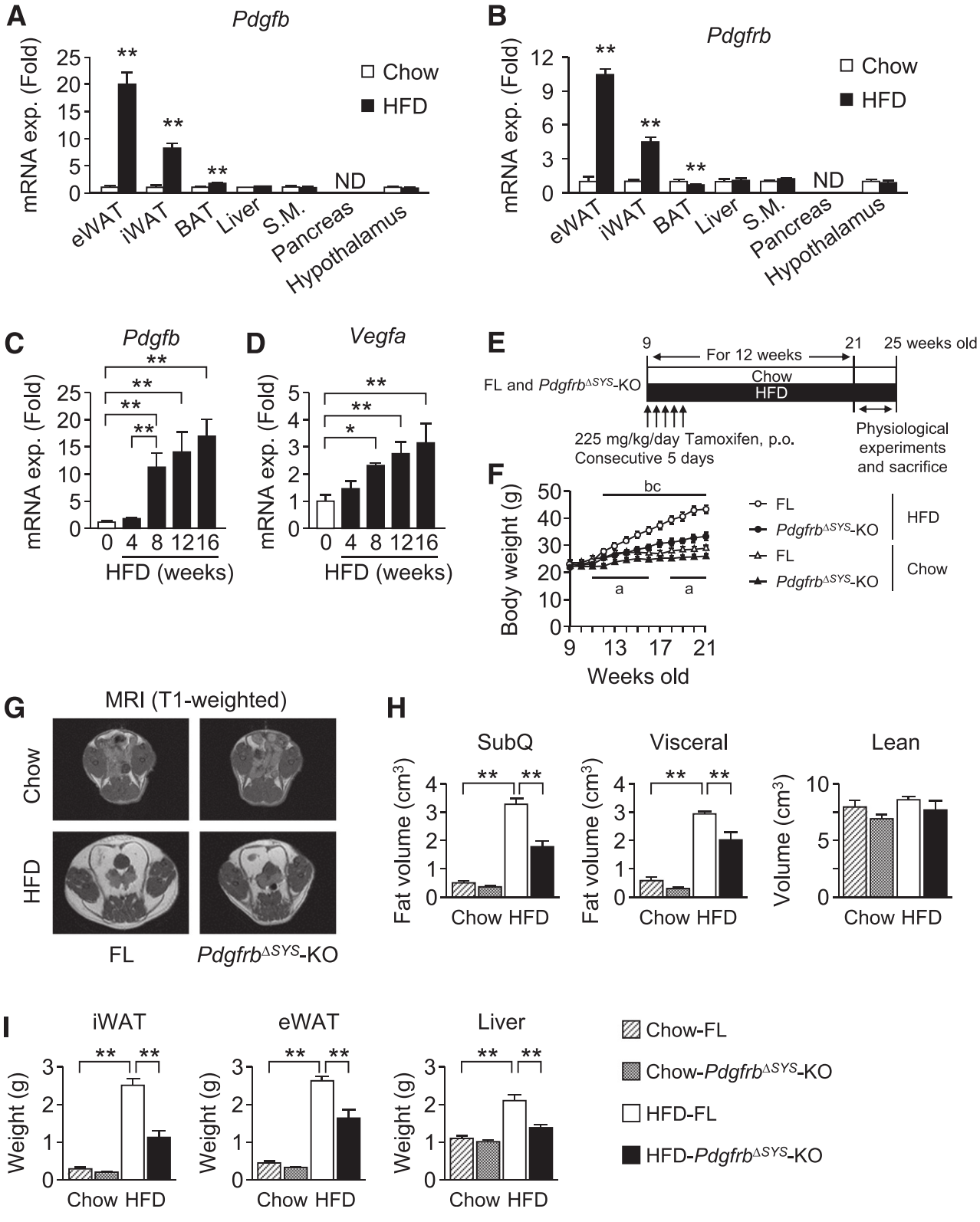

Figure 1—Systemic *Pdgfrb* KO mice exhibited resistance to diet-induced obesity. Mice were fed a chow diet or an HFD from 8 weeks of age. Influences of HFD feeding on mRNA levels of *Pdgfb* (*A*) and *Pdgfrb* (*B*) in various tissues of mice at 22–24 weeks old (n = 4–6 per group). The time course of changes in the mRNA levels of *Pdgfb* (*C*) and *Vegfa* (*D*) during HFD feeding (n = 5–6 per group). *E*: Protocol of tamoxifen administration and HFD feeding. At 9 weeks old, tamoxifen was administered to both *Cre-ER*/*Pdgfrb*$^{flox/flox}$ and *Pdgfrb*$^{flox/flox}$ mice to obtain *Pdgfrb*$^{\Delta SYS}$-KO mice and their tamoxifen-treated FL mice. Each genotype of mice was divided into two groups and fed a chow diet or an HFD. In vivo analyses of metabolic phenotypes were performed from 21 to 25 weeks of age, and then the mice were killed for tissue sampling. *F*: Changes in body weight in FL and *Pdgfrb*$^{\Delta SYS}$-KO mice during chow diet or HFD feeding. Representative images of MRI (T1-weighted image; *G*), and the estimated volumes of subcutaneous (SubQ) fat, visceral fat, and lean mass, assessed by MRI (*H*).

Statistical Analyses

Data are expressed as the mean ± SE. *P* values were obtained by an unpaired two-tailed Student *t* test between two groups and by two-way ANOVA with Bonferroni test among groups composed of two genetic strains (KO vs. FL) and two diets (chow diet vs. HFD). One-way ANOVA with Bonferroni test was used in Figs. 1*C* and *D*, 3*H*, 4*C*, and 5*C*, and Supplementary Figs. 2*E* and 4*C*. $P < 0.05$ was considered to be significant.

RESULTS

HFD-Induced Obesity Was Prevented in Mice Lacking *Pdgfrb*

We initially characterized the tissue expression profiles of PDGF-B and its receptors in lean and obese C57BL/6J mice. The mRNA of *Pdgfb* was markedly increased in the WAT of mice by HFD feeding but remained unchanged in the liver, muscle, and hypothalamus (Fig. 1*A*). The *Pdgfrb* tissue expression profile was almost the same as that of *Pdgfb* (Fig. 1*B*). A WAT-specific increase in the mRNA levels of *Pdgfb* and *Pdgfrb* appears to reflect the angiogenesis, since the expression of *Kdr*, a marker of ECs, increased only in eWAT but not in the liver and skeletal muscle after HFD feeding (Supplementary Fig. 1*A*). The expression of *Pdgfb* markedly increased after 8 weeks of HFD feeding and increased further thereafter (Fig. 1*C*). In contrast, the increase observed in the expression of *Vegfa* was more gradual and milder than that in *Pdgfb* (Fig. 1*D*). Serum PDGF-B levels slightly increased, whereas serum VEGF-A levels were not significantly affected by HFD feeding (Supplementary Fig. 1*B* and *C*). These results indicate that PDGF-B rather than VEGF-A was strongly produced in adipose tissue and acted in an autocrine and/or paracrine manner during the development of obesity in mice. To clarify whether the up-regulated expression of PDGF-B and PDGFRβ during the development of obesity is involved in adipose tissue expansion associated with impaired glucose metabolism, we investigated the influence of the deletion of *Pdgfrb* using a tamoxifen-inducible gene ablation system (21,22). The experimental protocol was illustrated in Fig. 1*E*. *Pdgfrb*$^{\Delta SYS}$-KO and FL mice were divided into two groups and maintained on a chow diet or an HFD. Although the congenital systemic KO of *Pdgfrb* resulted in embryonic lethality (18), *Pdgfrb*$^{\Delta SYS}$-KO mice survived and grew normally (data not shown). PDGFRβ mRNA levels and protein expression in WAT, brown adipose tissue, the liver, and skeletal muscle were significantly lower in *Pdgfrb*$^{\Delta SYS}$-KO mice than in FL mice, and the KO efficacy of PDGFRβ did not differ during HFD feeding (Supplementary Fig. 1*D–F*). Body weights were similar between the two genotypes prior to the administration of tamoxifen. Nevertheless, body weights were lower in *Pdgfrb*$^{\Delta SYS}$-KO mice than in FL mice under normal chow-fed condition (Fig. 1*F*). Furthermore, *Pdgfrb*$^{\Delta SYS}$-KO mice were protected from body weight gain and the accumulation of subcutaneous and visceral fat under HFD conditions (Fig. 1*F–I*). However, no significant changes in lean mass and muscle mass in hind limbs occurred in either genotype (Fig. 1*H* and Supplementary Fig. 1*G*). Consistent with the changes observed in fat volume, fasted serum levels of leptin were significantly lower in *Pdgfrb*$^{\Delta SYS}$-KO mice (20.8 ± 5.5 ng/mL) than in FL mice (47.1 ± 2.3 ng/mL) under HFD feeding condition. These results indicated that PDGFRβ signaling plays crucial roles in the regulation of fat accumulation.

Profiles of Adipocytes in Mice Lacking *Pdgfrb*

We analyzed the sizes of the adipocytes in the eWAT of FL and *Pdgfrb*$^{\Delta SYS}$-KO mice. Under HFD-fed conditions, adipocytes in eWAT were smaller in *Pdgfrb*$^{\Delta SYS}$-KO mice than in FL mice (Fig. 2*A–C*). To clarify the direct effects of the deletion of *Pdgfrb* on adipocyte differentiation, we isolated mouse embryonic fibroblasts (MEFs) from FL and *Pdgfrb*$^{\Delta SYS}$-KO mice (FL-MEF and KO-MEF) and compared their differentiation into adipocytes in vitro. Lipid accumulation was slightly higher in KO-MEF mice than in FL-MEF mice, although both were partial. Moreover, the mRNA levels of *Adipoq* were slightly higher, whereas those of *Leptin* and *Pparg* were significantly higher in KO-MEF mice (Supplementary Fig. 2*A–C*). However, mitogenic activity detected by MTT assay and analysis of insulin-stimulated Ki67 expression was lower in KO-MEF mice than in FL-MEF mice (Supplementary Fig. 2*D* and *E*). These results indicated that the lack of PDGFRβ in eWAT did not lead to reductions in body fat via the direct inhibition of adipocyte differentiation.

HFD-Induced Chronic Inflammation in eWAT Was Attenuated in Mice Lacking *Pdgfrb*

We subsequently investigated chronic inflammation in eWAT. The results of immunostaining analyses demonstrated that CD11c$^+$ macrophages were almost absent in the eWAT of both genotypes under chow-fed conditions (data not shown). In contrast, a cluster of CD11c$^+$ macrophages around dead adipocytes (i.e., a crown-like structure [CLS] was prominent in the eWAT of control FL mice fed an HFD). In addition, the infiltration of proinflammatory macrophages and CLS formation were markedly

I: Tissue weights at 23–25 weeks old. Data are represented as the mean ± SEM. n = 6–10 per group. *$P < 0.05$; **$P < 0.01$; [a]$P < 0.05$, chow-fed FL vs. chow-fed *Pdgfrb*$^{\Delta SYS}$-KO mice; [b]$P < 0.05$, chow-fed FL vs. HFD-fed FL mice; [c]$P < 0.05$, HFD-fed FL vs. HFD-fed *Pdgfrb*$^{\Delta SYS}$-KO mice. *H* and *I*: Closed bars, HFD-fed *Pdgfrb*$^{\Delta SYS}$-KO mice; dotted bars, chow-fed *Pdgfrb*$^{\Delta SYS}$-KO mice; hatched bars, chow-fed FL mice; open bars, HFD-fed FL mice. BAT, brown adipose tissue; exp., expression; iWAT, inguinal white adipose tissue; ND, not detectable; S.M., skeletal muscle.

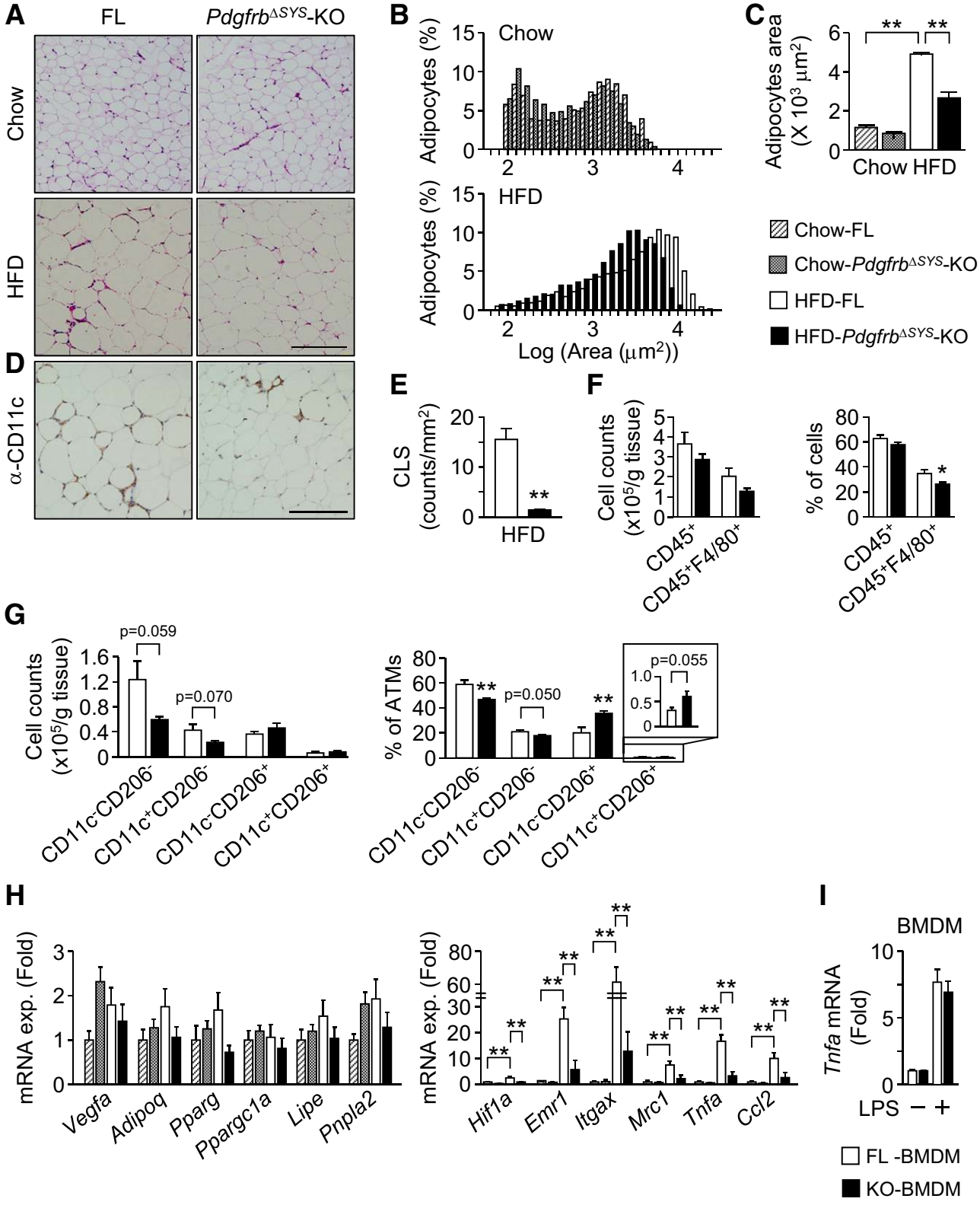

Figure 2—Suppressive effects of the *Pdgfrb* deletion on adipocyte enlargement and chronic inflammation in WAT in diet-induced obese mice. *A*: Representative hematoxylin-eosin staining of eWAT of control (*Pdgfrb*$^{flox/flox}$, FL) and *Pdgfrb*$^{\Delta SYS}$-KO mice. Scale bar, 200 μm. *B*: Frequency distribution of the adipocyte areas of eWAT of FL and *Pdgfrb*$^{\Delta SYS}$-KO mice fed a chow diet (top) and an HFD (bottom). *C*: Mean area of adipocytes (n = 4–8 per group). *D*: Representative images of eWAT immunostained with the anti-CD11c antibody. Scale bar, 200 μm. *E*: The number of CLSs. n = 6–8 per group. Flow cytometric analysis of the SVF in eWAT of HFD-fed mice. The number of macrophages (*F*) gated on CD45$^+$ or CD45$^+$F4/80$^+$ (left) and the percentage of total cells (right), and the number of subpopulation of macrophages (*G*) gated on CD11c$^-$CD206$^-$, CD11c$^+$CD206$^-$, CD11c$^-$CD206$^+$, or CD11c$^+$CD206$^+$ (left) and the percentage of adipose tissue macrophages (ATMs) in the SVF of eWAT (right) were analyzed (n = 6–7 per group). The inset shows the same data of

decreased in *Pdgfrb*$^{\Delta SYS}$-KO mice (Fig. 2*D* and *E*). In accordance with these histological observations, flow cytometric analyses clearly showed that total macrophages in the SVF of eWAT were decreased in *Pdgfrb*$^{\Delta SYS}$-KO mice fed an HFD (Fig. 2*F*). Furthermore, percentages of M1-macrophages defined by gating on CD11c^{+}CD206^{-} in CD45^{+}F4/80^{+} cells were decreased, whereas those of M2-macrophages defined by gating on CD11c^{-}CD206^{+} in CD45^{+}F4/80^{+} cells were significantly increased in *Pdgfrb*$^{\Delta SYS}$-KO mice (Fig. 2*G*).

In analyses of mRNA expression in eWAT from control FL and *Pdgfrb*$^{\Delta SYS}$-KO mice maintained on a chow diet or an HFD, no significant differences were observed in the expression levels of *Vegfa*, *Adipoq*, the adipogenic genes *Pparg* and *Ppargc1a*, or lipolytic genes *Lipe* and *Pnpla2* among the four groups (Fig. 2*H*). Regarding the hypoxic and inflammatory genes, the expression of *Hif1a*, *Emr1*, *Itgax*, *Mrc1*, *Tnfa*, and *Ccl2* was significantly increased by HFD feeding in FL mice, whereas the increasing effects were attenuated in HFD-fed *Pdgfrb*$^{\Delta SYS}$-KO mice (Fig. 2*H*). The expression of *Pdgfb* in the eWAT of *Pdgfrb*$^{\Delta SYS}$-KO mice was significantly lower than that of FL mice under HFD-fed condition (data not shown). These results indicated that HFD-induced chronic inflammation in eWAT was ameliorated in *Pdgfrb*$^{\Delta SYS}$-KO mice.

We further investigated the direct effects of the *Pdgfrb* deletion on the macrophage inflammatory response in vitro. The expression of the macrophage differentiation markers *Emr1*, *Itgax*, and *Mrc1* was similar between FL- and KO-BMDM (data not shown). Importantly, lipopolysaccharide-induced *Tnfa* expression was indistinguishable in both types of BMDMs (Fig. 2*I*). Therefore, the attenuation of chronic inflammation in *Pdgfrb*$^{\Delta SYS}$-KO mice appears to arise from the amelioration of fat accumulation rather than from the deletion of *Pdgfrb*, having a direct effect on macrophages.

Vascularity in eWAT Was Reduced in Mice Lacking *Pdgfrb*

Since the formation of a neovascular network is necessary for the development of adipose tissue, we investigated the vascularity of eWAT in FL and *Pdgfrb*$^{\Delta SYS}$-KO mice. The blood vessel area and number of branches were reduced by the deletion of *Pdgfrb* in chow-fed and HFD-fed conditions (Fig. 3*A*–*C*). The expression of VEGF receptor 2, a vascular endothelial marker, was increased by HFD feeding in the eWAT of FL mice, whereas no such increase was observed in *Pdgfrb*$^{\Delta SYS}$-KO mice (Supplementary Fig. 3). We confirmed that PDGFRβ was predominantly expressed in the SVF but not in the mature adipocyte fraction (MAF) of eWAT, particularly in the perivascular cells of pericytes (Fig. 3*D* and *E*). These cells also stained well with CD13 and neural/glial antigen 2 (NG2), recognized markers of pericytes. PDGF-B is an angiogenic factor that promotes the recruitment of pericytes to neovascular ECs for maturation via the activation of PDGFRβ in pericytes (15). Therefore, we investigated the ratio of the pericyte (green) association with ECs (red) as an index of vessel maturation and the angiogenic condition in eWAT (Fig. 3*F* and *G*), as previously described (32,33). Pericytes attached tightly along blood vessels (merged; yellow) in FL and *Pdgfrb*$^{\Delta SYS}$-KO mice under normal chow-fed condition. Importantly, we found that the attachment of pericytes was significantly reduced by HFD feeding in FL mice, indicating that these vessels were prone to vascular sprouting (33). To investigate the kinetics of HFD-induced pericyte behaviors, we measured the ratio of pericyte coverage in C57BL/6 mice fed an HFD for various periods (Fig. 3*H*). Pericyte-uncovered vessels increased by HFD feeding depending on the loaded period. On the other hand, the HFD-induced decrease in the pericyte coverage ratio was not observed in *Pdgfrb*$^{\Delta SYS}$-KO mice, and the ratio was similar to that in normal chow diet–fed FL mice (Fig. 3*F* and *G*). Interestingly, ECs with Ki67-stained nuclei were detected in some of the pericyte-uncovered areas in the eWAT of FL mice fed an HFD (Fig. 3*I*). The flow cytometry–based quantitative analysis again demonstrated that the mean fluorescent intensity of Ki67 in ECs was lower in *Pdgfrb*$^{\Delta SYS}$-KO mice than in FL mice (Fig. 3*J*). These results indicated that the HFD-induced detachment of pericytes from ECs and the subsequent proliferation of ECs, relevant to angiogenesis, appeared to be suppressed by the deletion of *Pdgfrb*.

To directly investigate whether PDGF-B induces pericyte detachment from mature vessels, we cultured whole eWAT from lean mice and treated it with PDGF-B for 24 h (Fig. 4*A* and *B*). CD13-labeled pericytes closely associated with the platelet endothelial cell adhesion molecule 1 (PECAM1)–stained vasculature in control tissues. The PDGF-B treatment caused their detachment from the vasculature in a dose-dependent manner (Fig. 4*A*–*C*). The vascular-detached pericytes were spindle shaped because of the lack of close contact with vessels (Fig. 4*B*). In contrast, in cultured adipose tissue from *Pdgfrb*$^{\Delta SYS}$-KO mice, where PDGFRβ-like immunoreactivity was lower than that from FL mice (Fig. 4*D* and *E*), PDGF-B–induced detachment of pericytes from the vasculature was significantly

CD11c^{+}CD206^{+} subpopulation at different *y*-scales. *H*: The mRNA expression of genes in eWAT. n = 4–10. *I*: *Tnfa* mRNA levels after the 3-h stimulation with lipopolysaccharide (0 or 1 ng/mL) under serum starvation for 4 h in BMDMs derived from FL (open bars) and *Pdgfrb*$^{\Delta SYS}$-KO mice (closed bars). n = 9 per group. Data represent the mean of three independent experiments. The mRNA expression was normalized to *Rn18s* and expressed as a fold change with the values for control. Data are represented as the mean ± SEM. $^{*}P < 0.05$ and $^{**}P < 0.01$. Closed bars, HFD-fed *Pdgfrb*$^{\Delta SYS}$-KO mice; dotted bars, chow-fed *Pdgfrb*$^{\Delta SYS}$-KO mice; hatched bars, chow-fed FL mice; open bars, HFD-fed FL mice. exp., expression; LPS, lipopolysaccharide.

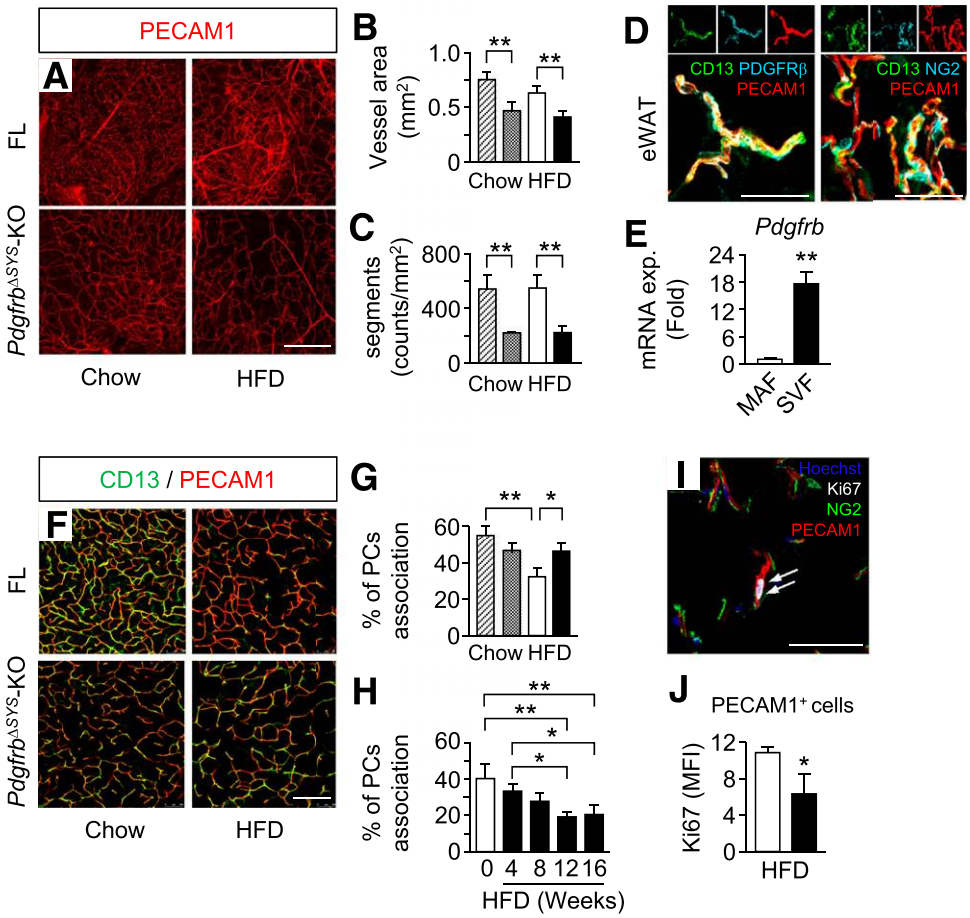

Figure 3—Effects of the *Pdgfrb* deletion on vascularity in WAT in mice. *A–C*: Changes in vascularity in eWAT of control (*Pdgfrb*$^{flox/flox}$, FL) and *Pdgfrb*$^{\Delta SYS}$-KO mice fed a chow diet and an HFD. The tip region of eWAT was used for vascular imaging. *A*: Representative vasculature of whole-mount eWAT. Blood vessels were visualized with anti-PECAM1 immunostaining. Scale bar, 500 μm. Quantitative vessel area (*B*) and numbers of vessel segments (*C*) analyzed with low-power field microscopy. To this end, the total PECAM-1–stained area and the numbers of branches of vessels on each microscopy (10× objective) were measured and averaged. n = 4 per group. *D*: Perivascular cells (pericytes [PCs]) in the eWAT of lean FL mice were costained with anti-CD13 (green) and anti-PDGFRβ (cyan, left panel) or anti-NG2 (cyan, right panel) in cryosections of eWAT. Blood vessels were visualized with anti-PECAM1 immunostaining. Scale bars, 50 μm. *E*: The mRNA expression levels of *Pdgfrb* in the MAF and SVF of eWAT in C57BL/6J mice. *F*: Representative whole-mount immunofluorescence images. eWAT of FL and *Pdgfrb*$^{\Delta SYS}$-KO mice fed a chow diet and an HFD was stained with anti-PECAM1 (red: ECs) and anti-CD13 antibodies (green: PCs). Scale bar, 200 μm. *G*: The percentage of PCs associating with blood vessels in panel *F*. *H*: Changes in the percentage of PCs associated with blood vessels in eWAT from C57BL/6 mice during HFD feeding. n = 4–5 per group. *I:* Representative immunofluorescence images stained with Hoechst (blue, nuclei), anti-Ki67 (white), NG2 (green), and PECAM1 (red) in eWAT of HFD-fed FL mice. The arrows indicate Ki67-positive nuclei of endothelial cells. Scale bar, 100 μm. *J*: The mean fluorescence intensity (MFI) of Ki67 in PECAM1$^+$ cells gated on CD45$^-$ in SVF of eWAT from HFD-fed FL and HFD-fed *Pdgfrb*$^{\Delta SYS}$-KO mice. n = 6–11 per group. Blood vessel areas (*A* and *B*) and pericyte associations (*F–H*) were measured with the ImageJ software. Data are represented as the mean ± SEM. *P < 0.05 and **P < 0.01. Closed bars, HFD-fed *Pdgfrb*$^{\Delta SYS}$-KO mice; dotted bars, chow-fed *Pdgfrb*$^{\Delta SYS}$-KO mice; hatched bars, chow-fed FL mice; open bars, HFD-fed FL mice. exp., expression.

attenuated (Fig. 4*F* and *G*). These results indicated that a high concentration of PDGF-B around vessels facilitates the detachment of pericytes from mature vessels through PDGFRβ signaling and promotes vascular remodeling in adipose tissue.

HFD-Induced Increments in PDGF-B in Adipose Tissue Originated From M1-Macrophages

To identify the cell types responsible for the marked increases observed in PDGF-B in obese adipose tissue, as shown in Fig. 1*A*, we initially analyzed the MAF and SVF separated from the eWAT of diet-induced obese mice. The expression of *Pdgfb* was significantly higher in the SVF than in MAF (Fig. 5*A*). To further clarify the cell types, we divided the SVF into CD45$^+$F4/80$^+$ macrophage and CD45$^-$F4/80$^-$ nonleukocyte populations that included ECs and preadipocytes. In the lean state, the expression of *Pdgfb* was similar between the two populations. In contrast, its expression was markedly increased in the macrophage fraction with obesity (Fig. 5*B*). Because ECs are known to play important roles in the maturation of vessels by producing PDGF-B (15,17), we analyzed the

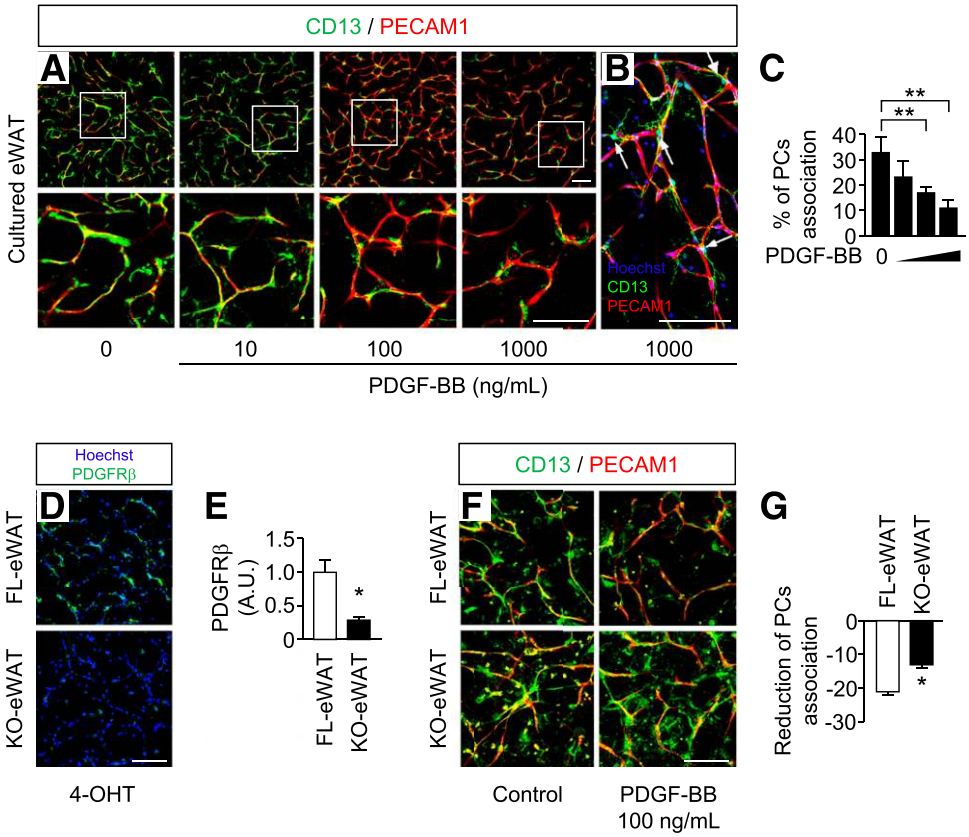

Figure 4—Changes in pericyte localization in cultured eWAT by an exogenous PDGF-BB treatment. Representative images of cultured eWAT stained with anti-CD13 (green) and anti-PECAM1 (red) antibodies (*A* and *B*) and counterstaining with Hoechst (*B*). Scale bars, 50 μm. The lower panels show a magnified view of the white squares in the top image. *B*: Representative high-magnification images in tissues treated with 1 μg/mL PDGF-BB for 24 h. *C*: Percentage of pericytes (PCs) associating with blood vessels analyzed under low-power field microscopy. $n = 6$ per group. *D–G*: The influence of the deletion of PDGFRβ on the PDGF-BB–induced changes in pericyte localization. Representative images of PDGFRβ (green)-positive cells (*D*) and mean fluorescence intensity of PDGFRβ-positive signals (*E*) to determine the KO efficiency in whole-mount cultured eWAT from *Cre-ER/Pdgfrb*$^{flox/flox}$ (KO-eWAT) and control mice (FL-eWAT) after treatment with 100 nmol/L 4-hydroxytamoxifen (4-OHT) for 48 h. $n = 3$ per group. *F*: Representative images of whole-mount eWAT from KO-eWAT and FL-eWAT stained with anti-CD13 (green) and anti-PECAM1 (red) antibodies after treatment with 100 ng/mL PDGF-BB for 24 h. *D* and *F*: Scale bars, 100 μm. *G*: The percentage of pericytes associated with blood vessels in panel *F*. $n = 9–11$ per group. Data represent the mean of independent experiments. Data are represented as the mean ± SEM. *$P < 0.05$ and **$P < 0.01$. A.U., arbitrary units.

content of ECs in SVF of eWAT from HFD-fed obese mice by different gating (Supplementary Fig. 4A and *B*). The expression of *Pdgfb* mRNA in the CD45$^-$CD31$^+$ ECs fraction was comparable to that in the CD45$^+$F4/80$^+$ macrophage fraction; however, most of the cells were in the CD45$^+$F4/80$^-$ and CD45$^+$F4/80$^+$ fractions, and ECs were a small component (only 1.1 ± 0.1%) of total SVF in obese eWAT.

We next examined the expression of *Pdgfb* in macrophage subpopulations in the eWAT of obese mice (Supplementary Fig. 4*C*). The *Pdgfb* expression was apparently high in F4/80$^+$CD11c$^+$CD206$^+$ macrophages; however, these cells were a small component (only 0.3 ± 0.1%) of total macrophages. In other fractions, CD11c$^+$CD206$^-$ M1-macrophages are a major type of cells expressing *Pdgfb*. In addition, the expression of *Pdgfb* was gradually and preferentially increased in F4/80$^+$CD11c$^+$CD206$^-$ M1-macrophages, but not in F4/80$^+$CD11c$^-$CD206$^+$ M2-macrophages in a time-dependent manner during HFD feeding (Fig. 5*C*), which appeared to correlate with pericyte detachment in the eWAT (Fig. 3*H*). Consistently, pericytes associated with vessels were further decreased around CLS areas compared with non-CLS areas in the obese adipose tissues (Supplementary Fig. 4*D* and *E*). These results suggested that the obesity-associated recruited M1-macrophages have a greater impact on the constitution of the high PDGF-B environment for vascular remodeling during adipose tissue enlargement.

HFD-Induced Ectopic Fat Deposition Was Reduced in Mice Lacking *Pdgfrb*

We examined lipid metabolism in each genotype of mice. Fasted serum nonesterified fatty acid, triglyceride, and cholesterol levels were not different between *Pdgfrb*$^{\Delta SYS}$-KO and FL mice being fed a chow diet but were significantly lower in *Pdgfrb*$^{\Delta SYS}$-KO mice than in FL mice being fed an HFD (Supplementary Table 3). HFD-induced accumulation of triglyceride in the quadriceps muscle and liver

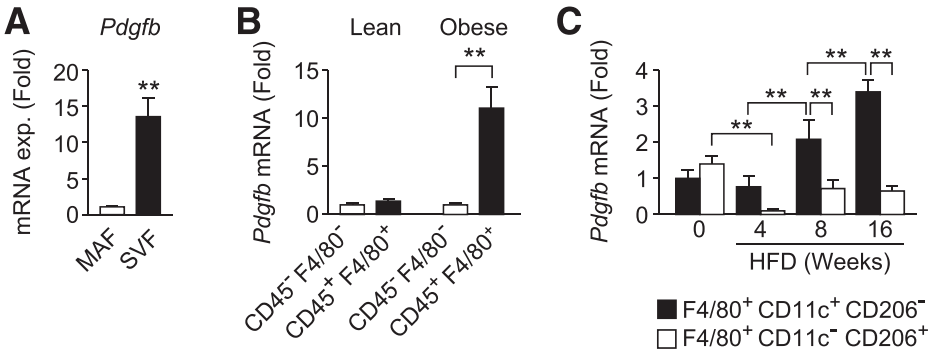

Figure 5—Identification of cell types strongly expressing *Pdgfb* in the eWAT of mice fed an HFD. Mice were maintained on an HFD from 8 weeks of age. *A*: mRNA levels of *Pdgfb* in the MAF and SVF isolated from the eWAT of C57BL/6J mice at 22 weeks old. *B*: The mRNA levels of *Pdgfb* in $CD45^-F4/80^-$ nonleukocyte populations and $CD45^+F4/80^+$ macrophages of the SVF from eWAT in FL mice before (Lean) and after (Obese) HFD feeding for 12 weeks. *C*: The time course of changes in the mRNA levels of *Pdgfb* in $F4/80^+CD11c^+CD206^-$ (closed bars) and $F4/80^+CD11c^-CD206^+$ cells (open bars) obtained from eWAT of C57BL/6J mice fed an HFD for indicated times. The mRNA expression was normalized to *Rn18s* and expressed as a fold change with the values for control. Data are represented as the mean ± SEM. n = 5–6 per group. $^{**}P < 0.01$. exp., expression.

was significantly reduced in $Pdgfrb^{\Delta SYS}$-KO mice, when compared with that in FL mice (Fig. 6*A* and *B*). In accordance with hepatic lipid contents, the results of histological analyses revealed brighter hepatocytes and more abundant vacuolar changes in the livers of HFD-fed FL mice, whereas these features of hepatic steatosis were ameliorated in $Pdgfrb^{\Delta SYS}$-KO mice (Fig. 6*C*). The hepatic expressions of lipogenic, β-oxidative, and gluconeogenic genes were significantly increased by HFD feeding in FL mice, whereas most of the increasing effects were attenuated in $Pdgfrb^{\Delta SYS}$-KO mice (Fig. 6*D*).

Energy Metabolism Was Enhanced in Mice Lacking *Pdgfrb*

Since HFD feeding did not cause ectopic fat accumulation in $Pdgfrb^{\Delta SYS}$-KO mice despite reduction in adipose tissue expansion, we investigated whether energy metabolism was enhanced in the mice. VO_2 and VCO_2 were higher both in the light and dark phases in $Pdgfrb^{\Delta SYS}$-KO mice than in FL mice under both chow diet and HFD conditions (Fig. 6*E* and *F*). Locomotor activity was also significantly higher in $Pdgfrb^{\Delta SYS}$-KO mice (Fig. 6*G*). Food intake was increased in the $Pdgfrb^{\Delta SYS}$-KO mice, possibly to compensate for the increased energy expenditure (Fig. 6*H*). In the inguinal WAT of $Pdgfrb^{\Delta SYS}$-KO mice, beige-related changes were not observed in the histological and RT-PCR analyses (Supplementary Fig. 5).

The HFD-Induced Impairment in Glucose Metabolism Was Prevented in Mice Lacking *Pdgfrb*

We investigated alterations in glucose metabolism in $Pdgfrb^{\Delta SYS}$-KO mice (Fig. 7*A*–*G*). Under chow-fed condition, glucose levels during GTT were significantly lower in $Pdgfrb^{\Delta SYS}$-KO mice than in FL mice, whereas no differences were observed in insulin levels during GTT and in glucose levels during ITT. HFD-induced glucose intolerance, hyperinsulinemia, and insulin resistance were more preventable in $Pdgfrb^{\Delta SYS}$-KO mice than in FL mice (Fig. 7*A*–*D*). Hyperinsulinemic-euglycemic clamp studies showed that the glucose infusion rate was markedly increased in $Pdgfrb^{\Delta SYS}$-KO mice in association with increases in the disappearance of whole-body glucose and the suppression of hepatic glucose production by insulin (Fig. 7*E*–*G*). We subsequently analyzed the insulin-induced phosphorylation of Akt in eWAT, the liver, and skeletal muscle of $Pdgfrb^{\Delta SYS}$-KO mice (Fig. 7*H*). Phosphorylation levels were reduced in all of these tissues in FL mice fed HFD. Importantly, reductions in phosphorylation levels in each tissue were prevented in $Pdgfrb^{\Delta SYS}$-KO mice fed an HFD. These results suggested that the deletion of PDGFRβ prevented HFD-induced insulin resistance in eWAT, the liver, and skeletal muscle.

We examined whether the deletion of *Pdgfrb* improved obesity and glucose metabolism, even after the development of obesity. The tamoxifen-induced deletion of *Pdgfrb* after 8 weeks of HFD feeding significantly decreased body weight gain and ameliorated insulin resistance in $Pdgfrb^{\Delta SYS}$-KO mice fed an HFD (Supplementary Fig. 6). Thus, the deletion of PDGFRβ had a therapeutic impact on existing obesity and its related metabolic abnormalities in mice.

DISCUSSION

WAT has a unique capacity for remodeling according to the energy status. Adequate angiogenesis is necessary for adipose tissue expansion because it enables the supplementation of nutrients and oxygen in newly enlarged areas. In the current study, we identified a distinguishing role for PDGF-B–PDGFRβ signaling in the regulation of the initiation on neovascular formation in WAT in diet-induced obesity. We found that the obesity-associated increase in PDGF-B promoted the detachment of pericytes from mature vessels, which was correlated with the

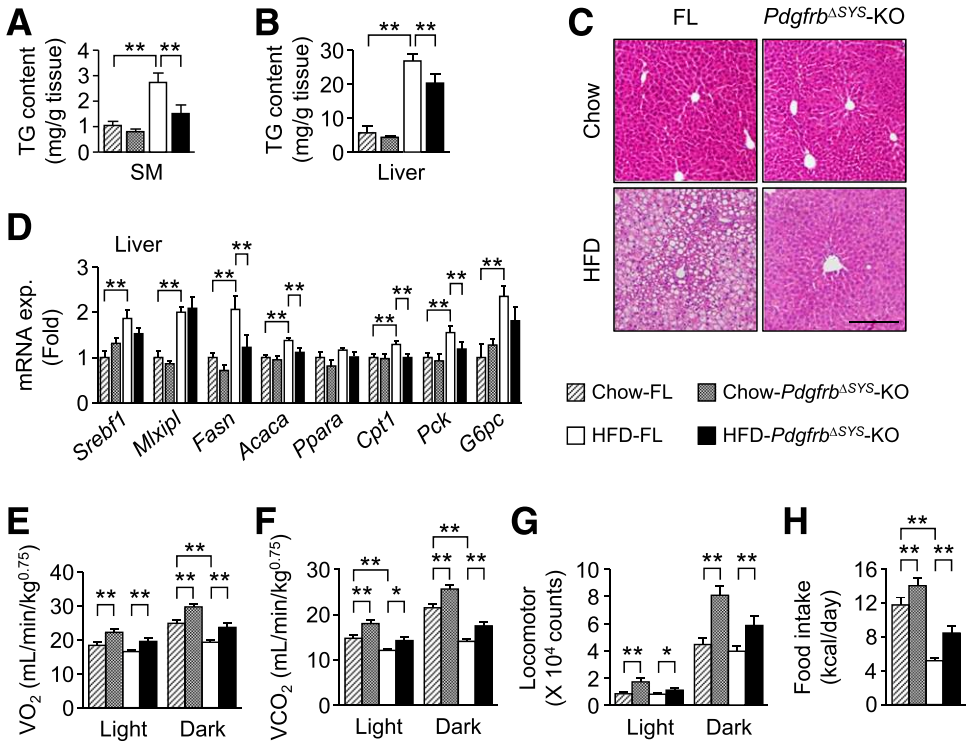

Figure 6—Deletion of systemic *Pdgfrb* reduced ectopic lipid accumulation in diet-induced obese mice. Chow-fed FL mice (hatched bars), chow-fed *Pdgfrb*$^{\Delta SYS}$-KO mice (dotted bars), HFD-fed FL mice (open bars), and HFD-fed *Pdgfrb*$^{\Delta SYS}$-KO mice (closed bars) were used. Total lipid content in the skeletal muscle (SM) (*A*) (n = 6–9 per group) and the liver (*B*) (n = 4–8 per group). Lipids were extracted by the method of Bligh-Dyer. Triglyceride (TG) contents among the total lipid content were measured using a triglyceride kit and normalized with each wet tissue weight. *C*: Representative hematoxylin-eosin staining in the liver. Scale bar, 200 μm. *D*: mRNA levels in the liver. n = 4–8 per group. Parameters of energy metabolism. Oxygen consumption (*E*), carbon dioxide production (*F*), locomotor activity (*G*), and daily food intake (*H*) were measured in mice at 19–21 weeks old by a metabolism measuring system. n = 6–9 per group. The mRNA expression was normalized to *Rn18s* and expressed as a fold change with the values for control. Data are represented as the mean ± SEM. $^{*}P < 0.05$ and $^{**}P < 0.01$. exp., expression.

proliferation of ECs in obese adipose tissue. In contrast, this detachment was attenuated and vascularity within WAT was reduced in *Pdgfrb*$^{\Delta SYS}$-KO mice. In addition, energy metabolism was increased in the mice. These appeared to contribute to the decreases in adipocyte size and chronic inflammation in *Pdgfrb*$^{\Delta SYS}$-KO mice even under HFD feeding conditions.

PDGFRβ is almost restrictively expressed in perivascular mural cells, and its signaling is known to be crucially involved in neovessel formation (14). Matured vasculature is covered with pericytes that are mobilized by PDGF-B secreted from ECs (34). The attached pericytes suppress the proliferation of ECs as well as the formation of new vascular branches (33–36); therefore, the detachment of pericytes from the vessel wall is considered to be the initial step in angiogenesis. In the current study, the ratio of pericytes attached to blood vessels was markedly decreased by HFD feeding in the eWAT of FL mice (Fig. 3). Our results strongly correlated with previous findings showing that the pericyte-to-EC ratio in adipose tissue was significantly lower in obese subjects than in lean subjects (37). Exogenous PDGF-B facilitated the detachment of pericytes from mature vessels via PDGFRβ signaling in tissue culture experiments (Fig. 4). In addition, some populations of ECs located at the site at which pericytes detached showed growth characteristics in obese adipose tissue (Fig. 3). Therefore, the vessels of obese adipose tissue may be anticipating vascular sprouting and angiogenesis. Since HFD-induced pericyte detachment was limited, HFD-induced angiogenesis and WAT expansion were attenuated in *Pdgfrb*$^{\Delta SYS}$-KO mice. These results suggested that obesity-induced angiogenesis in WAT largely depends on PDGF-B–PDGFRβ signaling in pericytes.

PDGF-B derived from ECs has been reported (14,38) to promote the proliferation of pericytes and/or their recruitment to blood vessels, whereas excessive PDGF-B derived from implanted tumor cells induced the recruitment of pericytes to tumor cells from neovessels (38,39). Thus, pericytes are considered to be recruited according to the concentration gradient of PDGF-B. We found that *Pdgfb* mRNA levels were similar between $CD45^{-}F4/80^{-}$ populations and $CD45^{+}F4/80^{+}$ macrophages in the eWAT of lean mice, whereas they selectively increased in $F4/80^{+}CD11c^{+}CD206^{-}$ M1-macrophages in the eWAT of obese mice (Fig. 5). Although ECs expressed *Pdgfb* mRNA, there were few ECs in SVF of the obese adipose

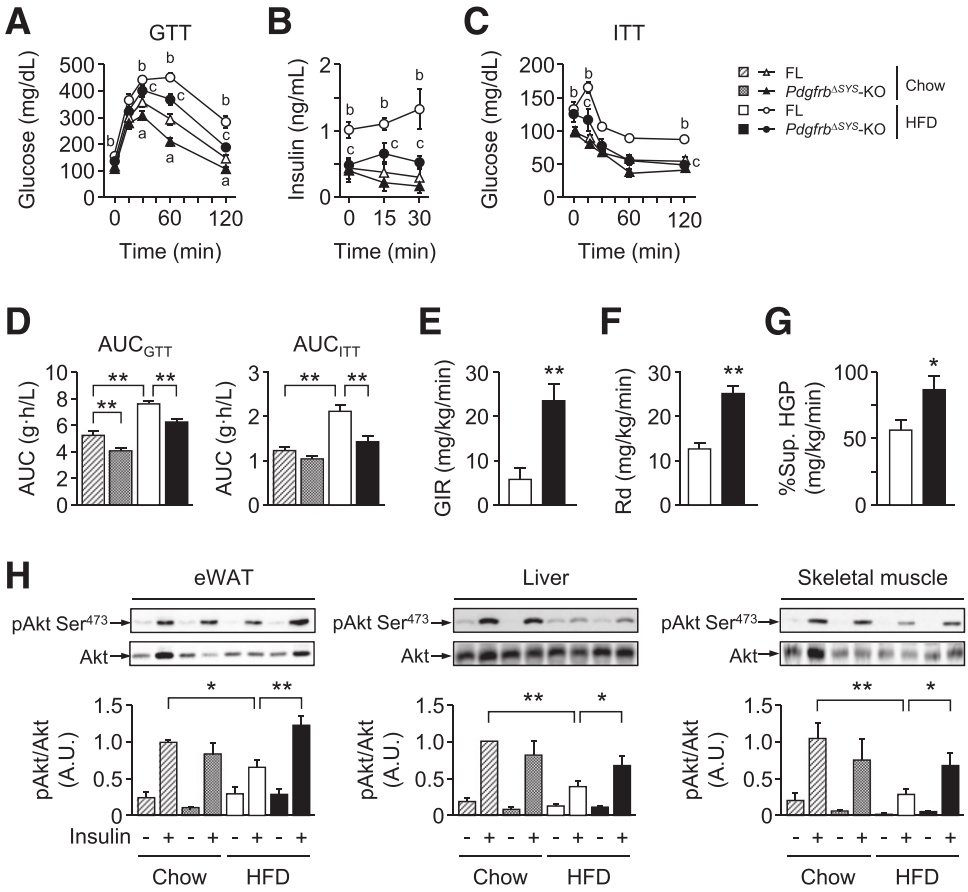

Figure 7— Deletion of systemic *Pdgfrb* improved glucose tolerance and insulin sensitivity in mice. Chow-fed FL mice (hatched bars), chow-fed *Pdgfrb*$^{\Delta SYS}$-KO mice (dotted bars), HFD-fed FL mice (open bars), and HFD-fed *Pdgfrb*$^{\Delta SYS}$-KO mice (closed bars) were used. Blood glucose (*A*) and insulin levels (*B*) during the GTT (n = 8–10 per group). *C*: ITT (n = 6–9 per group). $^{a}P < 0.05$, chow-fed FL vs. chow-fed *Pdgfrb*$^{\Delta SYS}$-KO mice; $^{b}P < 0.05$, chow-fed FL vs. HFD-fed FL mice; $^{c}P < 0.05$, HFD-fed FL vs. HFD-fed *Pdgfrb*$^{\Delta SYS}$-KO mice. *D*: Glucose area under the curve (AUC) in GTT (*A*) and ITT (*B*). *E–G*: Hyperinsulinemic-euglycemic clamp study in HFD-fed mice at 22 weeks old. Glucose infusion rate (GIR; *E*), glucose disposal rate (Rd; *F*), and the percentage suppression (%Sup.) of hepatic glucose production (HGP; *G*) in FL and *Pdgfrb*$^{\Delta SYS}$-KO mice under the 6-h fasting condition were examined. n = 6 per group. *H*: Representative Western blot images and quantitative results of insulin-induced Akt phosphorylation in eWAT, the liver, and skeletal muscle of FL and *Pdgfrb*$^{\Delta SYS}$-KO mice at 24 weeks old. n = 4–6 per group. Tissue samples were isolated 5 min after an intravenous injection of insulin (1.0 units/kg body wt) under the 6-h fasting condition. Data are represented as the mean ± SEM. $^{*}P < 0.05$ and $^{**}P < 0.01$. A.U., arbitrary units.

tissue (Supplementary Fig. 4*B*). On the basis of these results, we provide a putative model for explaining the regulation of WAT expansion by angiogenesis in obesity through PDGF-B–PDGFRβ signaling, as described in Fig. 8: PDGF-B produced by ECs appears to recruit pericytes toward the vessel walls to maintain the mature vascular system in the lean state. Under HFD feeding conditions, an excessive amount of PDGF-B is produced by infiltrated M1-macrophages in obese WAT. It may cause the detachment of pericytes from vessels via PDGFRβ signaling (i.e., an initial step in neovascular sprouting). The adipose tissue angiogenesis may help the WAT expansion because vascular remodeling enables the tissue to store abundant amounts of fuel provided by the HFD. Therefore, suppression of the PDGFRβ signaling may inhibit the detachment of pericytes from vessels within WAT and the tissue expansion, as observed in *Pdgfrb*$^{\Delta SYS}$-KO mice fed an HFD. However, it remained unclear whether the M1-macrophage–derived PDGF-B directly causes the detachment of pericytes from vessels and whether these events, if any, can sufficiently promote adipose tissue expansion. Further study is required to determine the causal relationship.

The M2-macrophage plays a principle role in angiogenesis, since it locates in the vicinity of the vessel branch and promotes angiogenesis by releasing proangiogenic factors, such as VEGF (40). In the current study, we found that M1-macrophage is a major source of PDGF-B in obese adipose tissue (Fig. 5). Although the *Pdgfb* mRNA was also highly expressed in the CD11c^{+}CD206^{+} macrophage, this subpopulation was almost negligible in the obese adipose tissue (Fig. 2*G* and Supplementary Fig. 4*C*); therefore, the functional significance of this type of macrophage remains to be clarified. Infiltration of M1-macrophage was also observed in the liver and muscle and contributes to the development of chronic inflammation in obesity (41,42); however, we did not detect any

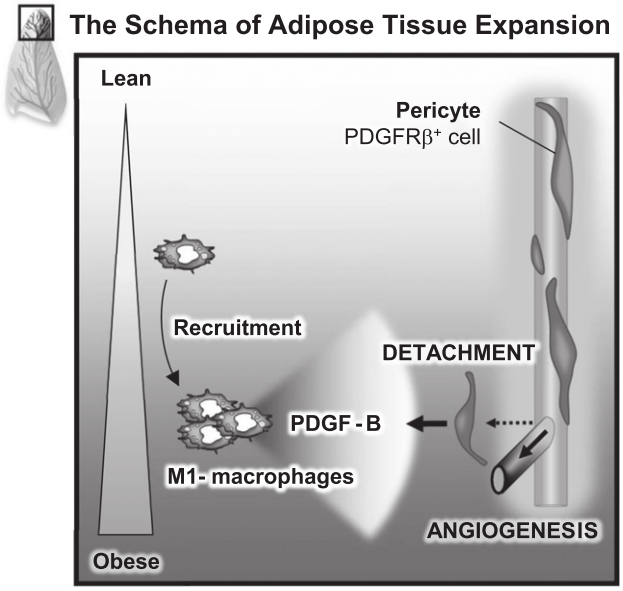

Figure 8—A conceptual model of vascular remodeling and adipose tissue expansion in adult obesity. Proinflammatory M1-macrophages increase along with adipose tissue expansion. They produce high levels of PDGF-B and promote the detachment of pericytes from mature vessels, thereby making vessels prone to sprouting. Consequently, adipose tissue angiogenesis continues with tissue enlargement.

increase in the expression of *Pdgfb* by HFD feeding in the liver and skeletal muscle of mice (Fig. 1). These results suggested that adipose tissue-specific environment, such as abnormal production of adipokines or hypoxia, promotes the production of PDGF-B in M1-macrophage in diet-induced obese mice. M1-macrophage may contribute to vascular remodeling in adipose tissue via PDGF secretion under obese conditions, whereas M2-macrophage may contribute to the development or maintenance of vascular system under physiological conditions.

Tamoxifen is widely used to generate inducible conditional transgenic mice; however, several recent studies (43,44) have been concerned with its influences on the adipocyte biology. In particular, acute adipocyte death and transient reduction of body weight have been observed during the tamoxifen treatment, although body weight was recovered by de novo differentiation of adipocytes after the treatment (43). In addition, tamoxifen has been reported to induce browning of subcutaneous fat (44). In the current study, we administered tamoxifen to all groups of mice, including FL mice, to conduct the experiments under the same condition. Body weight was not acutely changed during 5 days of tamoxifen treatment except in Supplementary Fig. 6, where tamoxifen was administered to obese mice. Moreover, we did not observe any histological feature of browning or increase of browning gene transcripts, such as *Ucp1*, in the inguinal WAT of both FL and $Pdgfrb^{\Delta SYS}$-KO mice (Supplementary Fig. 5). Thus, the influence of tamoxifen on metabolism in mice appeared to be negligible in the present experimental condition, although we cannot completely rule out the possibility that some phenotypes of $Pdgfrb^{\Delta SYS}$-KO mice might be affected by the treatment of tamoxifen, especially under the obese condition.

In obese adipose tissue, VEGF-A is mainly produced by mature adipocytes and promotes obesity-associated angiogenesis for the supply of oxygen and nutrients to hypoxic areas (11). Adipocyte-specific VEGF-A KO mice have dysfunctional adipose tissue with reduced vascular density (11). Thus, the obesity-associated production of VEGF-A in adipose tissue is crucial as the homeostatic machinery. In contrast, the present results indicated that PDGF-B was mainly produced by adipose tissue macrophages in obesity, particularly by proinflammatory M1-macrophages that infiltrated into the expanding tissues (Fig. 5). Therefore, it is possible to speculate that PDGF-B mediates pathological adaptation in obese adipose tissue. In this regard, the excess exposure of PDGF-B from infiltrated M1-macrophages to pericytes promotes inappropriate angiogenesis in obese adipose tissue, which may facilitate the further infiltration of immune cells (5), resulting in a disturbance in adipose tissue homeostasis.

The functional relationship between adipose tissue neovascularization and energy expenditure in obesity is somewhat complicated. The $Pdgfrb^{\Delta SYS}$-KO mice exhibited the limited adipose neoangiogenic capacity and enhanced energy metabolism; however, the primary mechanism responsible for reducing adiposity in the mice remains unknown. In addition, it is still unclear whether the observed changes in the adipose tissue vasculature of $Pdgfrb^{\Delta SYS}$-KO mice were due to primary effects of the *Pdgfrb* deletion or secondary effects of the lack of weight gain. Previous studies demonstrated that treatments with angiogenic inhibitors or antineovascular peptide not only inhibited adipose tissue enlargement but also enhanced energy metabolism (1,2,6), possibly by a compensatory mechanism for maintaining energy homeostasis. Therefore, we consider that insufficient expansion of adipose tissue, the main organ for energy storage, due to suppressed angiogenic activity might enhance energy metabolism in $Pdgfrb^{\Delta SYS}$-KO mice via unknown compensation pathways. Further studies are needed to clarify the precise underlying mechanism.

In conclusion, the current study demonstrated that the systemic deletion of *Pdgfrb* inhibited neovessel formation in WAT, reduced fat accumulation and chronic inflammation in visceral adipose tissue, and improved whole-body glucose metabolism in association with decreased ectopic fat deposition in the muscle and liver of diet-induced obese mice. We documented the distinct role of PDGF-B-PDGFRβ signaling in the development of adipose tissue neovascularization accompanied by diet-induced obesity. On the basis of these favorable effects, we consider the suppression of PDGF-B–PDGFRβ functions to be a valuable approach for preventing obesity and type 2 diabetes.

Acknowledgments. The authors thank Drs. S. Fujisaka, Y. Nishida, and K. Tobe, at the First Department of Internal Medicine, University of Toyama, and

Drs. M. Ikutani and Y. Nagai, at the Department of Immunobiology and Pharmacological Genetics, University of Toyama, for their technical advice regarding flow cytometry; Drs. S. Watanabe and K. Fujita, at the Division of Nutritional Biochemistry, Institute of Natural Medicine, University of Toyama, for their technical advice regarding lipids analysis; and T. Matsushima, at the Department of Pathology, University of Toyama, for her excellent technical assistance.

Funding. This research was supported by Promotion of Science Grants-in-Aid for Scientific Research (KAKENHI) grant 24591318 (to T.W.), a grant from the Japan Diabetes Foundation (to T.W. and T.S.), Takeda Science Foundation (to T.W.), Suzuken Memorial Foundation (to T.W.), The Hokuriku Bank Grant-in-Aid for Young Scientists (to T.W.), Research Grant from Mitsubishi Tanabe Pharma Corporation (to T.W.), The Murata Science Foundation (to T.W.), Foundation for Growth Science (to T.S.), and a Sasakawa Scientific Research Grant (to Y.O.).

Duality of Interest. No potential conflicts of interest relevant to this article were reported.

Author Contributions. Y.O. performed most of the experiments, designed the experiments, wrote the manuscript, and contributed to the discussion. T.W. conceived and designed the experiments, researched the data, wrote the manuscript, and contributed to the discussion. C.K., K.I., T.M., Y.In., K.K., and H.I. researched the data and contributed to the discussion. S.Y. and D.K. contributed to the discussion. Y.Is. and M.S. produced and provided *Pdgfrb*$^{\Delta SYS}$-KO mice and contributed to the discussion. H.T. and T.S. designed the experiments, wrote the manuscript, and contributed to the discussion. All authors critically reviewed the manuscript. T.W. and T.S. are the guarantors of this work and, as such, had full access to all the data in the study and take responsibility for the integrity of the data and the accuracy of the data analysis.

References

1. Rupnick MA, Panigrahy D, Zhang CY, et al. Adipose tissue mass can be regulated through the vasculature. Proc Natl Acad Sci U S A 2002;99:10730–10735
2. Kolonin MG, Saha PK, Chan L, Pasqualini R, Arap W. Reversal of obesity by targeted ablation of adipose tissue. Nat Med 2004;10:625–632
3. Ye J, Gao Z, Yin J, He Q. Hypoxia is a potential risk factor for chronic inflammation and adiponectin reduction in adipose tissue of ob/ob and dietary obese mice. Am J Physiol Endocrinol Metab 2007;293:E1118–E1128
4. Fujisaka S, Usui I, Ikutani M, et al. Adipose tissue hypoxia induces inflammatory M1 polarity of macrophages in an HIF-1α-dependent and HIF-1α-independent manner in obese mice. Diabetologia 2013;56:1403–1412
5. Cao Y. Adipose tissue angiogenesis as a therapeutic target for obesity and metabolic diseases. Nat Rev Drug Discov 2010;9:107–115
6. Bråkenhielm E, Cao R, Gao B, et al. Angiogenesis inhibitor, TNP-470, prevents diet-induced and genetic obesity in mice. Circ Res 2004;94:1579–1588
7. Elias I, Franckhauser S, Ferré T, et al. Adipose tissue overexpression of vascular endothelial growth factor protects against diet-induced obesity and insulin resistance. Diabetes 2012;61:1801–1813
8. Nishimura S, Manabe I, Nagasaki M, et al. Adipogenesis in obesity requires close interplay between differentiating adipocytes, stromal cells, and blood vessels. Diabetes 2007;56:1517–1526
9. Shimizu I, Aprahamian T, Kikuchi R, et al. Vascular rarefaction mediates whitening of brown fat in obesity. J Clin Invest 2014;124:2099–2112
10. Sun K, Wernstedt Asterholm I, Kusminski CM, et al. Dichotomous effects of VEGF-A on adipose tissue dysfunction. Proc Natl Acad Sci U S A 2012;109:5874–5879
11. Sung HK, Doh KO, Son JE, et al. Adipose vascular endothelial growth factor regulates metabolic homeostasis through angiogenesis. Cell Metab 2013;17:61–72
12. Robciuc MR, Kivelä R, Williams IM, et al. VEGFB/VEGFR1-induced expansion of adipose vasculature counteracts obesity and related metabolic complications. Cell Metab 2016;23:712–724
13. Gerhardt H, Golding M, Fruttiger M, et al. VEGF guides angiogenic sprouting utilizing endothelial tip cell filopodia. J Cell Biol 2003;161:1163–1177
14. Heldin CH, Westermark B. Mechanism of action and in vivo role of platelet-derived growth factor. Physiol Rev 1999;79:1283–1316
15. Andrae J, Gallini R, Betsholtz C. Role of platelet-derived growth factors in physiology and medicine. Genes Dev 2008;22:1276–1312
16. Uhl E, Rösken F, Sirsjö A, Messmer K. Influence of platelet-derived growth factor on microcirculation during normal and impaired wound healing. Wound Repair Regen 2003;11:361–367
17. Armulik A, Abramsson A, Betsholtz C. Endothelial/pericyte interactions. Circ Res 2005;97:512–523
18. Lindahl P, Johansson BR, Levéen P, Betsholtz C. Pericyte loss and microaneurysm formation in PDGF-B-deficient mice. Science 1997;277:242–245
19. Crosby JR, Seifert RA, Soriano P, Bowen-Pope DF. Chimaeric analysis reveals role of Pdgf receptors in all muscle lineages. Nat Genet 1998;18:385–388
20. Hellström M, Kalén M, Lindahl P, Abramsson A, Betsholtz C. Role of PDGF-B and PDGFR-beta in recruitment of vascular smooth muscle cells and pericytes during embryonic blood vessel formation in the mouse. Development 1999;126:3047–3055
21. Shen J, Ishii Y, Xu G, et al. PDGFR-β as a positive regulator of tissue repair in a mouse model of focal cerebral ischemia. J Cereb Blood Flow Metab 2012;32:353–367
22. Xue Y, Lim S, Yang Y, et al. PDGF-BB modulates hematopoiesis and tumor angiogenesis by inducing erythropoietin production in stromal cells. Nat Med 2011;18:100–110
23. Wada T, Miyashita Y, Sasaki M, et al. Eplerenone ameliorates the phenotypes of metabolic syndrome with NASH in liver-specific SREBP-1c Tg mice fed high-fat and high-fructose diet. Am J Physiol Endocrinol Metab 2013;305:E1415–E1425
24. Wada T, Onogi Y, Kimura Y, et al. Cilostazol ameliorates systemic insulin resistance in diabetic db/db mice by suppressing chronic inflammation in adipose tissue via modulation of both adipocyte and macrophage functions. Eur J Pharmacol 2013;707:120–129
25. Yonezawa R, Wada T, Matsumoto N, et al. Central versus peripheral impact of estradiol on the impaired glucose metabolism in ovariectomized mice on a high-fat diet. Am J Physiol Endocrinol Metab 2012;303:E445–E456
26. Sameshima A, Wada T, Ito T, et al. Teneligliptin improves metabolic abnormalities in a mouse model of postmenopausal obesity. J Endocrinol 2015;227:25–36
27. Kimura K, Yamada T, Matsumoto M, et al. Endoplasmic reticulum stress inhibits STAT3-dependent suppression of hepatic gluconeogenesis via dephosphorylation and deacetylation. Diabetes 2012;61:61–73
28. Xue Y, Lim S, Bråkenhielm E, Cao Y. Adipose angiogenesis: quantitative methods to study microvessel growth, regression and remodeling in vivo. Nat Protoc 2010;5:912–920
29. Cho CH, Koh YJ, Han J, et al. Angiogenic role of LYVE-1-positive macrophages in adipose tissue. Circ Res 2007;100:e47–e57
30. Ke M-T, Fujimoto S, Imai T. SeeDB: a simple and morphology-preserving optical clearing agent for neuronal circuit reconstruction. Nat Neurosci 2013;16:1154–1161
31. Fujisaka S, Usui I, Bukhari A, et al. Regulatory mechanisms for adipose tissue M1 and M2 macrophages in diet-induced obese mice. Diabetes 2009;58:2574–2582
32. Furuhashi M, Sjöblom T, Abramsson A, et al. Platelet-derived growth factor production by B16 melanoma cells leads to increased pericyte abundance in tumors and an associated increase in tumor growth rate. Cancer Res 2004;64:2725–2733
33. Schrimpf C, Teebken OE, Wilhelmi M, Duffield JS. The role of pericyte detachment in vascular rarefaction. J Vasc Res 2014;51:247–258
34. Carmeliet P. Angiogenesis in health and disease. Nat Med 2003;9:653–660
35. Jain RK. Molecular regulation of vessel maturation. Nat Med 2003;9:685–693

36. Potente M, Gerhardt H, Carmeliet P. Basic and therapeutic aspects of angiogenesis. Cell 2011;146:873–887
37. Pellegrinelli V, Rouault C, Veyrie N, Clément K, Lacasa D. Endothelial cells from visceral adipose tissue disrupt adipocyte functions in a three-dimensional setting: partial rescue by angiopoietin-1. Diabetes 2014;63:535–549
38. Abramsson A, Lindblom P, Betsholtz C. Endothelial and nonendothelial sources of PDGF-B regulate pericyte recruitment and influence vascular pattern formation in tumors. J Clin Invest 2003;112:1142–1151
39. Hosaka K, Yang Y, Seki T, et al. Tumour PDGF-BB expression levels determine dual effects of anti-PDGF drugs on vascular remodelling and metastasis. Nat Commun 2013;4:2129
40. Schmidt T, Carmeliet P. Blood-vessel formation: bridges that guide and unite. Nature 2010;465:697–699
41. Fink LN, Costford SR, Lee YS, et al. Pro-inflammatory macrophages increase in skeletal muscle of high fat-fed mice and correlate with metabolic risk markers in humans. Obesity (Silver Spring) 2014;22:747–757
42. Itoh M, Kato H, Suganami T, et al. Hepatic crown-like structure: a unique histological feature in non-alcoholic steatohepatitis in mice and humans. PLoS One 2013;8:e82163
43. Ye R, Wang QA, Tao C, et al. Impact of tamoxifen on adipocyte lineage tracing: inducer of adipogenesis and prolonged nuclear translocation of Cre recombinase. Mol Metab 2015;4:771–778
44. Hesselbarth N, Pettinelli C, Gericke M, et al. Tamoxifen affects glucose and lipid metabolism parameters, causes browning of subcutaneous adipose tissue and transient body composition changes in C57BL/6NTac mice. Biochem Biophys Res Commun 2015;464:724–729